Collapse and Revivals of Wave Packets in Optical Lattices

G. Raithel,[2] W. D. Phillips,[1] and S. L. Rolston[1]
[1]*National Institute of Standards and Technology, PHYS A167, Gaithersburg, Maryland 20899*
[2]*University of Michigan, 2071 Randall Laboratory, Ann Arbor, Michigan 48109-1120*
(Received 11 July 1997)

We study the effects of dispersion, tunneling, and dissipation on wave-packet oscillations resembling coherent states of atoms in optical lattices. The wave packets are prepared by suddenly shifting the lattice after equilibration of the atoms at the lattice sites. The atoms oscillate in the light-shift potential wells, which exert a force arising from photon redistribution between lattice beams. We measure the resultant periodic intensity exchange between the beams, obtaining information on the wave-packet evolution. We observe a strong impact of dissipation on the overall shape and the time of revivals, as well as a suppression of tunneling by weak magnetic fields. [S0031-9007(98)07414-6]

PACS numbers: 32.80.Lg, 32.80.Pj, 42.50.Vk

Wave-packet motion in a quantum system decays because of dissipation and dispersion. The irreversible loss of quantum coherence due to dissipation usually leads to decay of the wave packet, while dispersion in a discretely quantized system can lead to collapse followed by revival of the wave packet. Revivals are mostly familiar from wave packets of almost dissipation-free quantized systems, such as electrons in Rydberg atoms [1]. In the present paper we study center-of-mass (c.m.) wave packets of atoms in optical lattices, a periodic quantum system in which we encounter the intriguing situation of intertwined dispersive and dissipative wave-packet decay, allowing us to investigate the mutual interplay of these phenomena.

Optical lattices are periodic light-shift potentials for atoms, created by the interference of multiple laser beams, which cool and localize atoms at the lattice sites [2]. The anharmonicity of the potential wells in the lattices is a source of dispersion or spreading of wave packets. Dissipation arises from spontaneous emission, which introduces irreversible coherence loss. Recently, wave-packet motion of atoms in optical lattices has been observed using Bragg scattering [3–6] and recoil-induced resonance [7]. Complementary steady-state frequency-domain spectra exhibiting vibrational sidebands have also been obtained [8]. In these investigations, the decay of the wave packets and the width of the vibrational sidebands have been dominated by the anharmonicity-induced dispersion, so that only an upper limit on the rate of dissipative coherence decay could be obtained. The coherence decay rate is smaller than the photon scattering rate, because of: (1) the Lamb-Dicke effect [9], where localization of the atoms to much less than the optical wavelength reduces the fraction of photon scattering events that are inelastic and destroy the coherence; (2) the transfer of coherence, even upon inelastic photon scattering [10–12], a process whose efficiency depends on the harmonicity of the potential. In this paper we study wave packets in optical lattices at times long after their excitation, in regimes where dissipative coherence loss and the tunneling-induced curvature of bands are of equal or greater importance than anharmonicity-induced dispersion.

In the experiment, we employ a 1D lin$\perp$lin optical lattice [2], whose quantization direction z is parallel to the lattice beams. The light-shift potential wells are spaced by $\lambda/4$ and correspond to alternating σ^+ and σ^- polarizations. Cesium atoms are collected, cooled, and trapped in the lattice using the $6S_{1/2},\ F = 4 \rightarrow 6P_{3/2},\ F' = 5$ transition ($\lambda = 2\pi/k = 852$ nm, $\Gamma/2\pi = 5.2$ MHz). Prior to the wave-packet excitation the atoms reach steady-state, i.e., they mostly occupy the internal states $|m_F = \pm 4\rangle$ that correspond to the lowest adiabatic potential $U(z)$ of the lattice [2], and their rms position spread around the minima of $U(z)$ reaches $\approx 0.05\lambda$ [8]. Coherent-state-like c.m. wave packets are then generated by suddenly shifting the lattice by $0 < dz < 0.25\lambda$ using a phase modulator in one lattice beam. Semiclassically, all atoms then oscillate back and forth in the potential wells with the same phase, as they are acted on by the dipole force $F(z) = -\nabla U(z)$. The force results from photon transfer between the lattice beams via absorptions and stimulated emissions. The redistribution-induced power difference $\Delta P(t)$ between the two lattice beams depends on the dipole force and the number of atoms N as

$$\Delta P(t) = -Nc\langle \nabla U(x)\rangle = Nc\langle \dot{p}\rangle , \qquad (1)$$

$\langle\ \rangle$ denoting the ensemble average. Thus, we determine the momentum derivative $\langle \dot{p}\rangle(t)$ by measuring $\Delta P(t)$. Similar techniques have already been employed in Refs. [7,13,14].

We quantitatively model the experiment using Monte-Carlo wave-function simulations (QMCWF), which include all magnetic sublevels of $6S_{1/2},\ F = 4$, the hyperfine levels of the excited state $6P_{3/2}$, and c.m. quantization. The simulated wave functions allow us to calculate the difference $\Delta G(t)$ between the gains of

the two lattice beams induced by their interaction with a single atom:

$$\Delta G(t) \sim \mathrm{Im}\langle\psi_g|V_x e^{ikz} - V_y e^{-ikz}|\psi_e\rangle, \qquad (2)$$

$|\psi_e\rangle$ ($|\psi_g\rangle$) denoting the excited- (ground-) state part of the full atomic wave function V_x and V_y are the atom-field coupling operators for the corresponding polarizations of the lattice beams propagating in the $\pm z$ directions. In the limit of small relative power transfer $\Delta P(t)/P$, P denoting the power of each lattice beam, the experimentally observed power transfer $\Delta P(t)$ is proportional to $\Delta G(t)$.

Three typical experimental results are shown in Fig. 1. Using Eq. (1) and assuming a cloud of N Cs atoms generating a signal on a detector cross section of 1 mm^2 we find a maximum of the transfer ratio $|\Delta P/P|$ of $\approx 10^{-5}\frac{dz}{\lambda}\frac{\Gamma}{\delta}N$, valid for small dz and large detuning δ. With a typical MOT ($N \sim 10^7$) and close to resonance ($\delta \simeq -5\Gamma$) one could obtain $|\Delta P/P| \sim 50\%$. In such cases the atomic oscillations would not only depend on the laser parameters and dz, but also on the redistribution-induced oscillation of the light intensity inside the cloud of atoms. To avoid such higher-order effects, we used only about 10^5 atoms, as estimated from the size of the signal. The experimental and theoretical curves in Fig. 1 are in excellent agreement, except for a faster decay of the experimental data in the second half of the displayed time intervals. We attribute the faster experimental decay to laser intensity inhomogeneity. The initial collapse of the oscillations is due to anharmonicity-induced dephasing [3,8]. The revivals evident in Fig. 1 confirm recent suggestive observations [3,6]. Figure 1c demonstrates that magnetic fields can enhance the revival structures, as frequently observed in our experiments and verified by QMCWF (see below, discussion of Figs. 4 and 5).

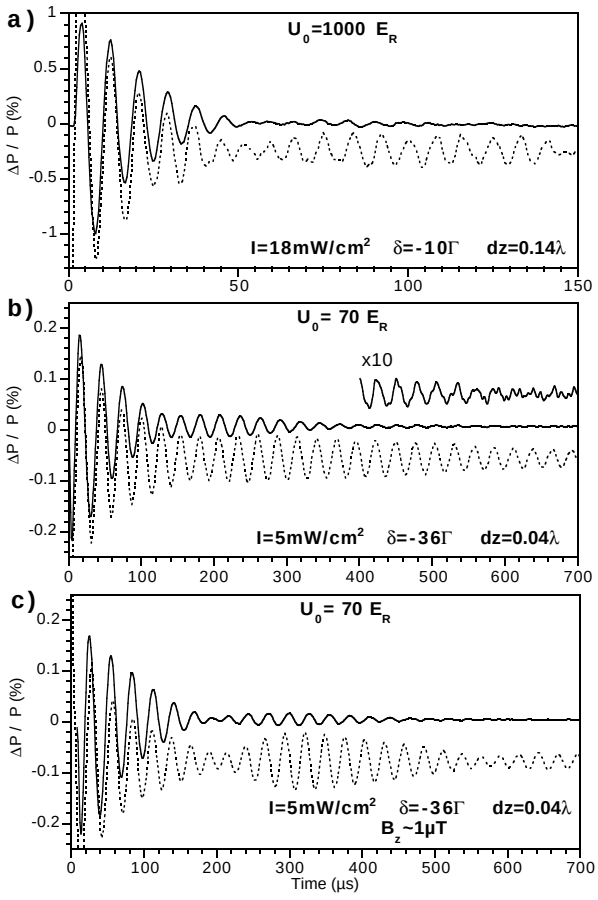

FIG. 1. Experimental (solid) and theoretical (dotted) power transfer ratio $(\Delta P/P)(t)$ induced by coherent-state-like wave-packet oscillations initiated by a sudden shift of the lattice at $t = 0$ by the indicated values of dz. For clarity, dotted and magnified lines are displaced. The theoretical results are obtained from QMCWF and are scaled to match the second extremum, because the first is strongly affected by the time constant of the shift. Panel (c) has an additional magnetic field in the z direction. The panels indicate the potential depth U_0 in units of the recoil energy $E_R = \hbar^2k^2/2m$.

We observe the expected dependence of the oscillation frequency $\propto\sqrt{U_0}$ (see Fig. 2) when we vary the magnitude U_0 of the potential depth. For constant lattice shift dz the number of oscillation periods during the initial collapse is approximately constant, consistent with the anharmonicity of the self-similar potential being the main reason for the initial signal collapse [3]. For constant δ and atomic wave packets [15], it is concluded from Eq. (1) and confirmed by our quantum model that the maximum transfer ratio $|(\Delta P/P)(t)|$ does not depend on U_0. This behavior is seen in Fig. 2 for $U_0 \geq 120E_R$. A moderate decrease, observed for $U_0 = 1250E_R$ and greater, is due to adiabatic effects caused by the nonzero time constant of the lattice shift. At $U_0 = 60E_R$ the signal is smaller because shallow potentials are less effective at trapping atoms, implying a lower degree of localization of the atomic distribution prior to the sudden lattice displacement.

In the remainder of the paper we analyze the revivals we observe past the time scale imposed by the anharmonicity-induced dephasing. Although the dynamics of atoms in optical lattices can be reasonably well

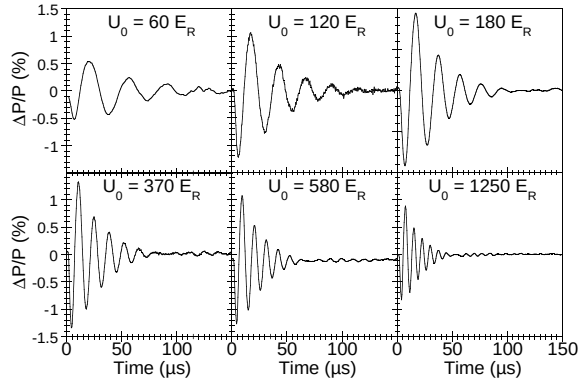

FIG. 2. Power transfer ratio $\Delta P/P$ induced by coherent-state-like wave-packet oscillations for $\delta = -10\Gamma$ and the indicated values of U_0. At $t = 0$ the lattice is shifted by $dz = 0.14\lambda$.

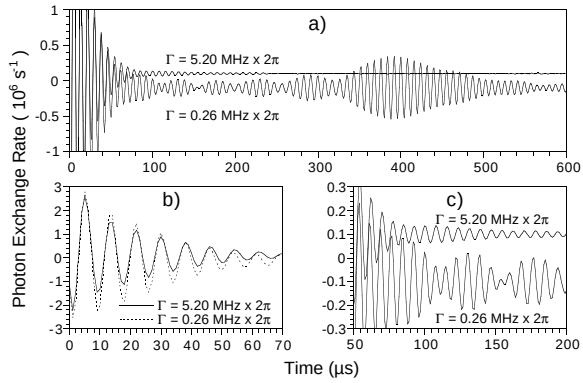

FIG. 3. Wave-packet signals obtained from QMCWF with $I = 18$ mW/cm^2 and $\delta = -52$ MHz. The lattice is shifted by $dz = 0.14\lambda$ with a $1/e$ time constant of $\tau = 3$ μs. The excited-state decay rates are as indicated. For clarity, some curves are offset from zero.

described by motion of a localized atom in a single potential well, the proper description of our periodic quantum system uses the basis of Bloch states, whose energies are bands $E_\upsilon(q)$, where q is the quasimomentum, $-k < q < k$, and υ the band index. Evaluating Eq. (2) in that basis, we find that the wave-packet signal mostly arises from coherences between states with band indices differing by one, which is the type of coherence found in coherent-state-like wave packets. The wave-packet signal solely arises from coherences between states having the same q; these are the only coherences in the system. The bands which can be identified with well-defined vibrational states in the lattice potential wells (tightly bound bands) are sufficient to understand most of the wave-packet dynamics, since most atoms reside in these bands [2]. Because of anharmonicity, the average energy difference between neighboring bands decreases with υ, causing *vibrational dispersion, i.e., interband dispersion* of wave packets. We observe in our QMCWF that in our lattice type the atoms occupy all quasimomenta q with the same probability. Therefore, the tunneling-induced widths of the bands manifest themselves as continuous spreads of the coherence oscillation frequencies. Thus, tunneling causes *intraband dispersion*.

The simplest revival structure occurs if dissipative coherence loss can be neglected, and the revivals are not affected by the tunneling-induced bandwidths. Then the bands become fixed vibrational energy levels E_υ. Considering the lowest-order anharmonic correction associated with our sinusoidal potential $\propto -\sin^2(2kz)$, we find $E_\upsilon \approx \hbar\omega(\upsilon + 1/2) + E_R\,\upsilon^2/2$, E_R denoting the recoil energy. This series of energy levels produces vibrational (interband) dispersion and causes a revival of coherent-state-like wave packets at $T_R = h/E_R = 500$ μs. A simulated approximation to that simple case is shown in the lower curves of Fig. 3, where parameters are as in Fig. 1a, except that an excited-state decay rate $\Gamma' = 0.05\Gamma = 260$ kHz $\times\, 2\pi$ is assumed. The dissipation only weakly affects the initial, anharmonicity-induced dephasing process (Fig. 3b), but it completely destroys the full revival that is observed at $\sim$400 μs in the weakly damped case. We attribute the fact that the revival occurs at $\sim$400 μs and not at 500 μs to higher-order anharmonicity. Since Γ is so high, we never measured wave packets similar to the weakly damped case of Fig. 3, not even at larger detunings, but quite frequently we measure revivals at early times, e.g., at $\sim$100 μs in Fig. 1a. In the vicinity of that time, the weakly damped case of Fig. 3 displays intermediate structures that are totally changed by dissipation, as shown in Fig. 3c. The slight amplitude maximum at about 110 μs, observed in the strongly damped case of Fig. 3, is the only leftover that is reminiscent of the revival seen in Fig. 1a. Differences between theory and experiment are presumably caused by the time dependence of the lattice shift and imperfections of the optical alignment.

In Figs. 1b and 1c the potentials are only $70E_R$ deep, and under absence of magnetic fields the tunneling width of the $\upsilon = 3$ bands [16], which is the highest one carrying significant population, is 4.7 kHz (see Figs. 4 and 5, left). Thus, tunneling-induced (intraband) dispersion becomes important after roughly 200 μs. To see the significance of tunneling in our model, we can artificially eliminate tunneling by replacing the energies of the predominantly populated bands by the respective average band energies. In a further step, we can also eliminate the anharmonicity by replacing the average band energies by a harmonic sequence. Figure 5 shows the results of these manipulations for lattice parameters such as in Fig. 1b. The left panel of Fig. 5, which shows the band populations vs time, proves that the manipulations do not affect the steady-state populations and the population redistribution after the lattice shift. Thus, the modifications of the wave-packet signals, shown in the right panel of Fig. 5, are not due to changes in the performance of laser cooling, but solely due to modified evolution of the coherences. A

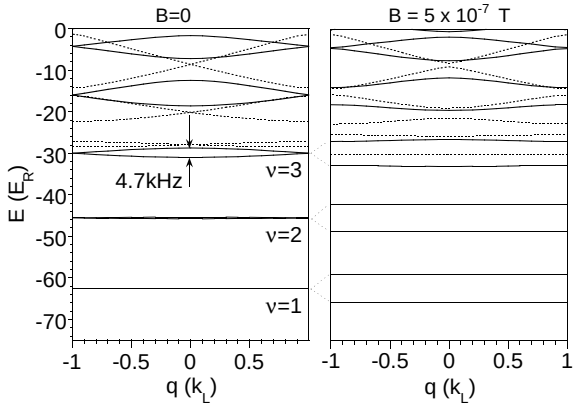

FIG. 4. Band structure for lattice parameters such as in Fig. 1b and the indicated magnetic fields in z direction. Solid (dotted) lines correspond to internal states with even (odd) magnetic quantum numbers.

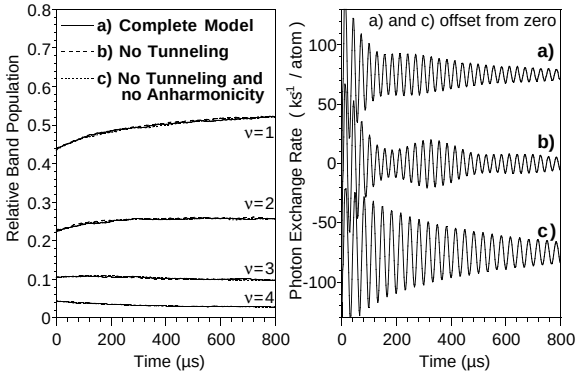

FIG. 5. Populations of the indicated bands n (left) and signals of coherent-state-like wave packets (right) obtained from QMCWF with the lattice parameters as in Fig. 1b and (*a*) no manipulations, (*b*) no tunneling and (*c*) no tunneling and no anharmonicity; the manipulations in (*b*) and (*c*) are explained in the text. In the left panel, the three curves shown for each band are almost indistinguishable.

comparison of curves (*b*) and (*c*) in Fig. 5 demonstrates that anharmonicity-induced dispersion (i.e., interband dispersion) leads to dephasing within about five cycles, and introduces a revival at $\approx 300\ \mu$s, which is the beat time between the two lowest vibrational coherences. Tunneling-induced intraband dispersion largely washes out that revival [compare curves (*a*) and (*b*) in Fig. 5]. To our satisfaction, the curve corresponding to the full model reproduces the experimental result best.

As shown in Fig. 1c, a weak magnetic field in z direction can be used to "re-establish" this revival. Though having no influence on the average oscillation frequencies of the coherences, the weak magnetic field removes the quasidegeneracy between the bandpairs found for $B = 0$ [16]. As a result, the tunneling turns from resonant into nonresonant, causing a strong reduction of tunneling rates and bandwidths, as seen in Fig. 4. A similar effect in double-well potentials has been studied in Ref. [17]. The bandwidth reduction makes the system almost equal to the artificial situation labeled (b) in Fig. 5, which displays a revival similar to the one in Fig. 1c.

In summary, we have studied wave-packet motion in a system exhibiting comparable dispersion and dissipation effects. We observed unexpectedly early revivals and, with the aid of QMCWF simulations, find that dissipation strongly influences the nature of the revivals. Such anomalous revivals could be a general feature of dispersive quantum systems with state-dependent coherence decay rates. Tunneling is found to have a clear impact on wave-packet motion in shallow optical lattices. The impact is reduced by weak magnetic fields in the z direction, which remove tunneling resonances.

This work was partially supported by the U.S. Office of Naval Research and by NSF Grant No. PHY-9312572. G. Raithel acknowledges support by the Alexander-von-Humboldt Foundation.

[1] J. Yeazell, M. Mallalieu, and C. R. Stroud, Phys. Rev. Lett. **64**, 2007 (1990).
[2] P. S. Jessen and I. H. Deutsch, Adv. At. Mol. Phys. **37**, 95 (1996), and references therein.
[3] G. Raithel, G. Birkl, A. Kastberg, W. D. Phillips, and S. L. Rolston, Phys. Rev. Lett. **78**, 630 (1997).
[4] G. Raithel, G. Birkl, W. D. Phillips, and S. L. Rolston, Phys. Rev. Lett. **78**, 2928 (1997).
[5] P. Rudy *et al.*, Phys. Rev. Lett. **78**, 4906 (1997).
[6] A. Görlitz, M. Weidemüller, T. W. Hänsch, and A. Hemmerich, Phys. Rev. Lett. **78**, 2096 (1997).
[7] M. Kozuma, K. Nakagawa, W. Jhe, and M. Ohtsu, Phys. Rev. Lett. **76**, 2428 (1996).
[8] M. Gatzke, G. Birkl, P. Jessen, A. Kastberg, S. L. Rolston, and W. D. Phillips, Phys. Rev. A **55**, R3987 (1997).
[9] R. H. Dicke, Phys. Rev. **89**, 472 (1953).
[10] C. Cohen-Tannoudji, J. Dupont-Roc, and G. Grynberg, *Atom-Photon Interactions* (J. Wiley & Sons, Inc., New York, 1992).
[11] J. Y. Courtois and G. Grynberg, Phys. Rev. A **46**, 7060 (1992).
[12] W. D. Phillips and C. I. Westbrook, Phys. Rev. Lett. **78**, 2676 (1997).
[13] J. Soeding *et al.*, Europhys. Lett. **20**, 101 (1992).
[14] C. Triche *et al.*, in *Proceedings of the Conference on Ultracold Atoms and Bose-Einstein Condensation*, edited by K. Burnett (Optical Society of America, Washington, DC, 1996), p. 82.
[15] The steady-state position distribution of atoms in optical lattices does not depend on the laser parameters if, as in Fig. 2 for $U_0 \geq 120E_R$, the steady-state temperature of the atoms follows $k_B T \propto U_0$ [8], implying a thermal vibrational occcupation number $\langle n \rangle \sim \sqrt{U_0}$.
[16] For $B = 0$, the two sets of potential wells with σ^+ and σ^- polarization support degenerate sets of vibrational states, resulting in two, almost degenerate bands for each quasibound vibrational state. Magnetic fields in z direction separate the band pairs into two distinct bands.
[17] S. Ya. Kilin, P. R. Berman, and T. M. Maevskaya, Phys. Rev. Lett. **76**, 3297 (1996).